VOLUME 113, NUMBER 17
AUGUST 14, 1991

JOURNAL
OF THE
AMERICAN
CHEMICAL
SOCIETY

A Study of the Structure and Dynamics of Dimethyloctadecylsilyl-Modified Silica Using Wide-Line ^2H NMR Techniques

Robert C. Zeigler† and Gary E. Maciel*

Contribution from the Department of Chemistry, Colorado State University, Fort Collins, Colorado 80523. *Received July 12, 1990*

Abstract: The structure and dynamics of dimethyloctadecylsilyl-modified silica gel (C_{18}-silica) were studied by using solid-state ^2H NMR techniques. In order to reproduce with a theoretical model the ^2H line shapes that were observed for the C_{18}-silica samples, it was necessary to assume that a variety of environments are present on the C_{18}-silica surface and that this heterogeneity results in different details of the motion of silane groups that are bonded to different regions of the C_{18}-silica surface. ^2H spectra that were taken on the C_{18}-silica samples at temperatures below room temperature appear to be superpositions of two line shapes, indicating that some silane groups move with a simple two-site jump motion, along with others that move with a more complex distribution of motions. At −50 °C, the addition of wetting liquids can affect the ^2H line shape; different liquids can have dramatically different effects on the observed ^2H line shapes. Simple surface structures for C_{18}-silica are proposed that are consistent with the NMR data observed in this study.

Introduction

Modified silicas are commonly used as stationary phases in both liquid chromatography and gas chromatography.[1,2] Recently, modified silica surfaces in which the surface-modifying groups are chemically bound to the silica surface have become very popular because of their great stability, particularly at high temperatures.

By far the most commonly used types of liquid chromatographic stationary phases are the alkylsilyl silicas.[2] Dimethyloctadecylsilyl-modified silica (C_{18}-silica) is a representative and very popular member of this class of useful chromatographic stationary phases. A key to the continued development of new and useful chromatographic separations with this type of stationary phase is a fundamental understanding of the surface conformations and dynamics of the alkylsilyl moieties, as well as an understanding of the interactions between C_{18}-silica and solvent/solute systems.

Many techniques have been used to study these kinds of materials. The most commonly used technique is the correlation of chromatographic performance with changes in the composition of the chromatographic stationary phase.[3-5] Fluorescence has also been used to study the dynamics in silyl-modified silica systems.[6,7]

Nuclear magnetic resonance spectroscopy has proven to be a very useful technique for the study of chromatographic stationary phases.[8-26] ^{13}C NMR spectroscopy has been used to study species

* To whom correspondence should be addressed.
† Present address: HIMONT Research & Development Center, 800 Greenbank Road, Wilmington, DE 19808.

(1) Grushka, E.; Kikta, E. J., Jr. *Anal. Chem.* **1977**, *49*, 1004A.
(2) *Bonded Stationary Phases in Chromatography*; Grushka, E., Ed.; Ann Arbor Science Publishers: Ann Arbor, MI, 1974.
(3) Schunk, T. C.; Burke, M. F. *Int. J. Environ. Anal. Chem.* **1986**, *25*, 81.
(4) Morel, D.; Serpinet, J. *J. Chromatogr.* **1982**, *248*, 231.
(5) Lochmuller, C. H.; Wilder, D. R. *J. Chromatogr. Sci.* **1979**, *17*, 574.
(6) Carr, J. W.; Harris, J. M. *Anal. Chem.* **1986**, *58*, 626.
(7) Beufils, J. P.; Hennion, M. C.; Rosset, R. *Anal. Chem.* **1985**, 2593.
(8) Gay, I. D. *J. Phys. Chem.* **1974**, *78*, 38.
(9) Kaplan, S.; Resing, H. A.; Waugh, J. S. *J. Chem. Phys.* **1973**, *59*, 5681.
(10) Kohler, J.; Chase, D. B.; Farlee, R. D.; Vega, A. J.; Kirkland, J. J. *J. Chromatogr.* **1986**, *352*, 275.
(11) Akapo, S. O.; Simpson, C. F. *J. Chromatogr. Sci.* **1990**, *28*, 186.
(12) Jinno, K. *J. Chromatogr.* **1989**, *27*, 729.
(13) Bayer, E.; Albert, K.; Reiners, J.; Nieder, M.; Muller, D. *J. Chromatogr.* **1983**, *264*, 197.

0002-7863/91/1513-6349$02.50/0

adsorbed on silica surfaces[8-10] and to distinguish different silane structures bound to silica surfaces.[11-14] The dynamics of *n*-alkylsilyl silicas have been studied by using the cross-polarization time constant, T_{CH}, and the ^1H or ^{13}C spin–lattice relaxation time constant, T_1.[13-26] Another NMR approach that has been used to study the dynamics of alkylsilyl-modified silica is observation of the effects of motion on NMR line shapes. The general principle behind NMR line shape analysis is that molecular motion changes the shape of and, in general, narrows an NMR peak that is otherwise broadened by such effects as chemical shift anisotropy, the heteronuclear dipolar interaction, or the quadrupolar interaction. Line shape analysis of ^{13}C NMR resonances broadened by chemical shift anisotropy showed that carbons near the unbound ends of silica-bound *n*-alkylsilyl chains are either more mobile or are structurally more homogeneous than the bound ends of the chains and are influenced by the composition of wetting liquids.[19,21] A wide-line ^2H NMR study of alkoxysilyl-modified silica showed that motion of the alkoxysilyl groups persisted at temperatures as low as −150 °C and that the addition of liquids to the modified silica surface had limited effects on the mobilities of the alkoxysilyl groups.[27]

We have chosen to study the surface structure and dynamics of selectively deuterated C_{18}-silica by wide-line ^2H NMR. Preliminary ^{13}C NMR studies of the system showed that differences exist in the C_{18}-silica system as a result of differences in surface coverage and the presence of wetting liquids.[23,24] A detailed ^{13}C NMR study of the C_{18}-silica system was carried out concurrently with the work reported here; those results are reported elsewhere.[25,26]

Experimental Section

Synthesis of C_{18}-Silicas and Solvent-Modified C_{18}-Silicas. All solvents that are specified to be "dry" were reagent grade materials distilled from a sodium–benzophenone mixture under N_2(g). Gas chromatography was used to analyze the products of every synthesis step.

Synthesis of [1,1-d_2]Dimethyloctadecylchlorosilane. Reduction of Methyl Stearate to [1,1-d_2]Stearyl Alcohol. A 38.74-g portion of methyl stearate (Aldrich, 99%, dried over $CaCl_2$) in 100 mL of dry ethyl ether (Mallinckrodt, analytical reagent grade, distilled from sodium + benzophenone) was added dropwise to 3.3 g of $LiAlD_4$ (MSD, 99.9%, used as received) in 200 mL of dry ethyl ether with rapid stirring by a magnetic stir bar under N_2(g), with cooling from an ice bath.[28] After the addition of all of the methyl stearate solution, the reaction flask was stirred for 1 h to ensure that the reduction reaction was complete. A 10-mL portion of H_2O was added dropwise to the reaction solution, and then the ether solution was poured slowly into 50 mL of ice–water. After separation of the ether–water mixture, the ether phase was washed with 250 mL of an aqueous 10% H_2SO_4 solution, followed by two 50-mL aliquots of H_2O. The ether phase, which contained the [1,1-d_2]stearyl alcohol, was then dried overnight over $CaCl_2$.

Conversion to [1,1-d_2]Stearyl Acetate and Pyrolysis To Form [1,1-d_2]-1-Octadecene.[29] The [1,1-d_2]stearyl alcohol/ether solution from the previous reaction step was filtered to remove the $CaCl_2$, and 30 mL of acetyl chloride was added; after 15 min, the resulting [1,1-d_2]stearyl acetate solution was distilled to a pot temperature of 100 °C at 0.050 Torr to remove the ether and excess acetyl chloride from the product. The pyrolysis of the pot residue, mainly [1,1-d_2]stearyl acetate, was carried out at 500 °C in a vertical tubular reactor (1.5 cm in internal diameter, 40 cm long, filled with glass helices), with a slow N_2 flow (about 0.1 cm^3 N_2/s) maintained through the reactor in a direction parallel to the [1,1-d_2]stearyl acetate flow. Four passes through the pyrolysis reactor at a rate of 1 drop/s were required to convert 80% of the [1,1-d_2]stearyl acetate to [1,1-d_2]-1-octadecene, which was collected at 0 °C. After each of the four passes through the pyrolysis reactor, the pyrolysis product was evacuated to 0.050 Torr at 25 °C to remove the acetic acid byproduct before the product mixture was again added to the top of the pyrolysis reactor. The [1,1-d_2]-1-octadecene was fractionally distilled at 180–200 °C under N_2 at 690 Torr. The distillate (19.4 g) was shown by gas chromatographic analysis to be >95% 1-octadecene; the 60-MHz ^1H NMR spectrum of the product showed no evidence of protons in the 1-position of the [1,1-d_2]-1-octadecene product.

Hydrosilylation of [1,1-d_2]-1-Octadecene.[30] To the [1,1-d_2]-1-octadecene product of the previous step were added under N_2(g) a 0.2-mL aliquot of 0.068 g of chloroplatinic acid (Aldrich, 99%) dissolved in a 10% solution of 2-propanol (Mallinckrodt, ACS grade) in dry ethyl ether and then, slowly, 12.5 mL of dimethylchlorosilane (Petrarch, distilled under N_2 immediately before use). After the addition of all of the dimethylchlorosilane, the reaction mixture was refluxed for 1.5 h before the [1,1-d_2]DMODCS product (19.7 g) was distilled at 150–175 °C and 0.050 Torr. The liquid-sample ^2H NMR spectrum of the [1,1-d_2]-DMODCS product showed only one resonance at a chemical shift of 0.8 ppm. Cumulative yield for the entire synthesis based on methyl stearate was 45%.

Synthesis of [9,10-d_2]DMODCS. Reduction of Methyl Oleate to [9,10-d_2]Methyl Stearate. A flask attached to a vacuum/H_2/D_2 manifold system equipped with a mercury manometer, containing a 2.58-g sample of tris(triphenylphosphine)rhodium(I) chloride (Aldrich, used as received), was alternately evacuated and then twice filled with H_2 (Alphagaz, prepurified, dried with a $CaSO_4$ bed). A 225-mL portion of dry benzene (Mallinckrodt, ACS) and 25 mL of absolute ethanol (Aaper Alcohol and Chemical Co., used as received) were added to the flask, which was then evacuated until the solvents in the reactor were observed to boil, then alternately filled with H_2, and evacuated twice more. After evacuation, the flask was filled to a pressure of 50 Torr above ambient with deuterium gas (MSD, 99.5(+) D_2, used as received). Then, 45 min after addition of 1 mL of cyclohexene, a gas chromatographic analysis of the reactor solution showed that all of the cyclohexene (Mallinckrodt, ACS grade) had been reduced. A 50-g portion of methyl oleate (Sigma, 99%) was added with a syringe. After a reaction period of 21 h with vigorous stirring at room temperature while the D_2 pressure in the reactor was maintained above ambient, the [9,10-d_2]methyl stearate product (46.86 g) was separated from the solvents and the catalyst residue by distillation at 160–170 °C and 0.050 Torr.

Synthesis of [9,10-d_2]-C_{18}-Silica. The [9,10-d_2]methyl stearate product of the previous reduction step was reduced to [9,10-d_2]stearyl alcohol with $LiAlH_4$, by using the procedure described above for the $LiAlD_4$ reduction of methyl stearate. The subsequent conversion of the [9,10-d_2]stearyl alcohol to [9,10-d_2]DMODCS was carried out as described above for the synthesis of [1,1-d_2]DMODCS. The cumulative yield of [9,10-d_2]DMODCS was 34%, based on methyl oleate. Liquid-sample ^2H NMR spectroscopy (Bruker/IBM-200 spectrometer) revealed only one peak for the [9,10-d_2]DMODCS (1.2 ppm).

Silica Silylation. The alkylsilyl silica samples were prepared by adding a solution of the appropriate [d_2]dimethyloctadecylchlorosilane in dry toluene to silica gel (Fisher S-679, evacuated at 0.020 Torr for 16 h at 180 °C prior to reaction) and then heating the mixture to 110 °C for 48

Table I. "Liquid" Loading Levels on C_{18}-Silica Samples[a]

silane loading level	liquid[b]	g solvent added/g silica
low[b]	water	0.076
low	acetonitrile	0.181
low	cyclohexane	0.112
high[c]	water	0.033
high	acetonitrile	0.016
high	cyclohexane	0.068

[a] Measured gravimetrically on nondeuterated C_{18}-silicas. [b] Loading levels of low-loading C_{18}-silica, 64 mg/g. [c] Loading levels of high-loading C_{18}-silica, 207 mg/g.

(14) Bayer, E.; Paulus, A.; Peters, B.; Laupp, G.; Reiners, J.; Albert, K. *J. Chromatogr.* **1986**, *364*, 25.
(15) Sindorf, D. W.; Maciel, G. E. *J. Am. Chem. Soc.* **1983**, *105*, 1848.
(16) Albert, K.; Evers, B.; Bayer, E. *J. Magn. Reson.* **1985**, *62*, 428.
(17) Gangoda, M.; Gilpin, R. K.; Fung, B. M. *J. Magn. Reson.* **1987**, *74*, 134.
(18) Gilpin, R. K.; Gangoda, M. E. *Talanta* **1986**, *33*, 176.
(19) Gilpin, R. K.; Gangoda, M. E. *J. Magn. Reson.* **1985**, *64*, 408.
(20) Gilpin, R. K.; Gangoda, M. E. *Anal. Chem.* **1984**, *56*, 1470.
(21) Gangoda, M. E.; Gilpin, R. K. *J. Magn. Reson.* **1983**, *53*, 140.
(22) Gilpin, R. K.; Gangoda, M. E. *J. Chromatogr. Sci.* **1983**, *21*, 35.
(23) Zeigler, R. C.; Maciel, G. E. *Chemically Modified Surfaces. Vol. 2: Chemically Modified Surfaces in Science and Industry*; Leyden, D. E.; Collins, W. T., Eds.; Gordon and Breach Science Publishers: New York, 1988; pp 319–336.
(24) Maciel, G. E.; Zeigler, R. C.; Taft, R. K. *Chemically Modified Surfaces. Vol. 1: Silanes, Surfaces and Interfaces*; Leyden, D. E., Ed.; Gordon and Breach Science Publishers: New York, 1986; pp 413–429.
(25) Zeigler, R. C. Ph.D. Dissertation, Colorado State University, 1989.
(26) Zeigler, R. C.; Maciel, G. E. *J. Phys. Chem.*, submitted for publication.
(27) Kelusky, E. C.; Fyfe, C. A. *J. Am. Chem. Soc.* **1986**, *108*, 1746.
(28) Gaylord, N. G. *Reduction with Complex Metal Hydrides*; Interscience: New York, 1956; pp 391–531.
(29) DuPuy, W. E.; King, R. W. *Chem. Rev.* **1960**, *60*, 431.
(30) Speier, J. L. *Adv. Organometal. Chem.* **1979**, *17*, 407.

h. Each reaction mixture was then cooled and rinsed three times with dry toluene; then the excess toluene was removed by heating the sample at 100 °C and 0.020 Torr for 16 h. The synthesis and all subsequent handling of the modified silica samples were carried out under dry $N_2(g)$. The alkylsilyl loading levels were determined gravimetrically.

The low-loading [1,1-d_2]-C_{18}-silica was synthesized by using 2.014 g of outgassed silica plus a solution of 0.233 g of [1,1-d_2]DMODCS in 3.5 mL of dry toluene to yield silylated silica with a loading level of 69 mg silane/g silica. The high-loading C_{18}-silica was synthesized by adding 4.185 g of [1,1-d_2]DMODCS in 1.6 mL of dry toluene to 2.078 g of dry silica. The silane loading level for this sample was 195 mg silane/g silica. The low-loading [9,10-d_2]-C_{18}-silica product had a silane loading level of 70 mg silane/g silica, while the high-loading [9,10-d_2]-C_{18}-silica sample had a 218 mg silane/g silica loading level.

Solvent Addition to C_{18}-Silica Samples. The solvent loading level of each deuterated C_{18}-silica sample investigated is listed in Table I; each of the deuterated C_{18}-silica samples was allowed to equilibrate for at least 24 h between solvent addition and any NMR experiment. These solvent loading levels are equal to the equilibrium loading levels that were previously determined for ^{13}C NMR study of analogous nondeuterated C_{18}-silicas.[25,26]

^2H NMR Spectroscopy. The ^2H NMR spectra were obtained at 92.1 MHz on a Bruker AM-600 NMR spectrometer that was modified for wide-line ^2H NMR spectra by the addition of a 1000-W radio frequency amplifier, a home-built high-speed digitizer (1 complex data point/0.8 μs), and a home-built probe. The quadrupole echo technique[31] was used to record all of the ^2H spectra, with a delay period (τ) of 50 μs unless otherwise specified. The sum of 20 000 repetitions was used for each of the high-loading samples; 50 000 repetitions were used for each of the low-loading samples. A 5-kHz exponential window function was used for all of the low-loading [1,1-d_2]-C_{18}-silica spectra and of the low-loading [9,10-d_2] samples at −50 °C. A 3 kHz, exponential window function was used for all of the spectra of the high-loading [1,1-d_2]-C_{18}-silica samples and all of the high-loading [9,10-d_2] samples at −50 °C. A 1-kHz exponential function was used for the 25 °C spectra of the [9,10-d_2] samples.

Deuterium Line Shape Simulations. All of the deuterium line shape simulations used in this paper were generated by using the program MXQET.[32,33] The simulated free induction decay output from each MXQET simulation was converted into a data format compatible with the FTNMR data manipulation program,[34] for exponential multiplication and other manipulations of the simulated spectra.

The simulations of the line shape distributions that were calculated by using the "dist P_g model" (vide infra) were done by summing a series of FID's, each of which was generated from MXQET. A distribution function such as a Gaussian or γ distribution[35] was used to calculate a set of normalized populations for each of the 42 simulated FID's that were used in the line shape calculation. Each of these FID's, which represents a Pake pattern of a given width, was weighted by the normalized intensity for that FID, as described by the distribution function, and then summed to generate the simulated FID for the distribution. This simulated final FID was Fourier-transformed and plotted, by using the FTNMR program. The FID's simulated in this manner were multiplied by the same exponential weighting factors as the experimentally gathered ^2H NMR data.

Results and Discussion

Background on ^2H Line Shapes. By limiting the discussion of quadrupolar nuclei to the case of ^2H nuclei in aliphatic compounds, one can assume that the energy and consequently the frequency associated with the quadrupolar interaction are much smaller (≤200 kHz) than those associated with the Larmor interaction (92 MHz), and the quadrupolar interaction can be treated as a perturbation. If this assumption is made, then the nuclear electric quadrupole effect can be represented in terms of a frequency shift:[36]

$$\pm\nu_Q = \tfrac{3}{8}\frac{e^2qQ}{h}(3\cos^2\Theta - 1 - \eta\sin^2\Theta\cos 2\phi) \qquad (1)$$

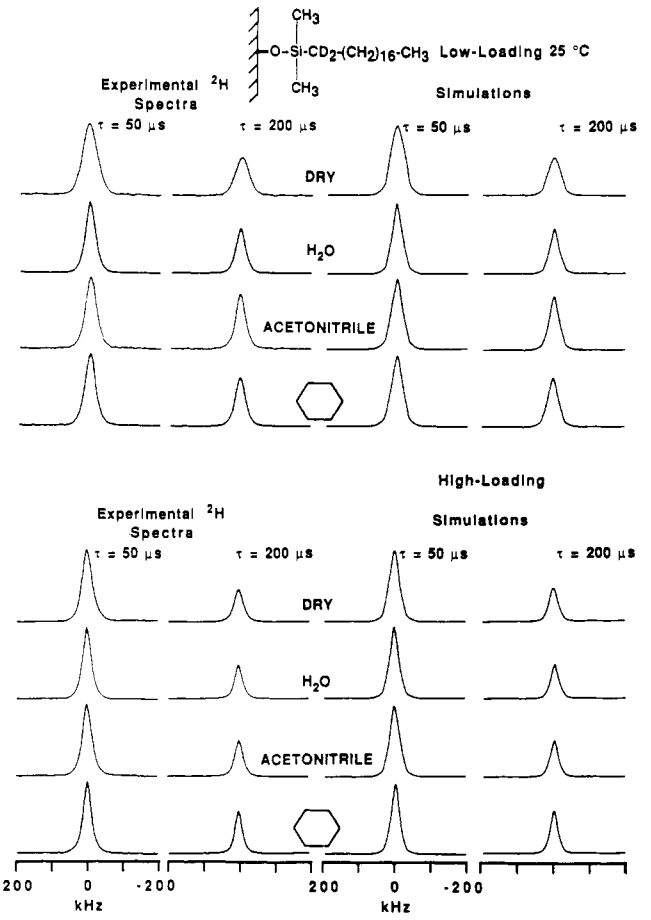

Figure 1. Comparison of simulated ^2H NMR spectra with the experimental spectra of low-loading and high-loading [1,1-d_2]-C_{18}-silica taken at room temperature. The parameters for these simulations can be found in Table VI.

In eq 1, e^2qQ/h is the nuclear electric quadrupole coupling constant, and Θ and ϕ define the orientation of the static magnetic field $\mathbf{B}_0$ in the principal axes system of the electric field gradient tensor at the quadrupolar nucleus; η is the asymmetry factor and can vary from 0 to 1.[37] For a powder sample, the $3\cos^2\Theta - 1 - \eta\sin^2\Theta\cos 2\phi$ term must be averaged over all transient orientations if the molecule is in motion and summed over all initial orientations (instantaneous orientations in a powder). The ± character of eq 1 indicates that two NMR resonances (corresponding to the $-1 \leftrightarrow 0$ and $0 \leftrightarrow 1$ transitions) are expected for any given orientation of the C–^2H internuclear vector relative to $\mathbf{B}_0$. The static electric field gradient tensor relevant to the ^2H nucleus in an aliphatic structure can be treated as an axially symmetrical tensor in which the unique axis is parallel to the C–^2H internuclear vector; i.e., the asymmetry factor (η) is equal to 0.[36] The wide-line ^2H NMR spectrum of a static solid is a Pake pattern with a full width of 250 kHz. Molecular motion will generally narrow the line shape and may introduce values of η between 0 and 1.[38]

^2H NMR Spectra of C_{18}-Silica. Wide-line ^2H NMR spectra were obtained on C_{18}-silicas deuterated in either of two different positions on the C_{18} chain. The samples are [1,1-d_2]-C_{18}-silica (I)

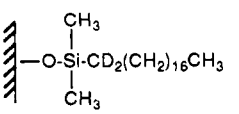

I

(31) Solomon, I. *Phys. Rev.* **1958**, *110*, 61.
(32) Greenfield, M. S.; Ronemus, A. D.; Vold, R. L.; Vold, R. R.; Ellis, P. D.; Raidy, T. E. *J. Magn. Reson.* **1987**, *72*, 89.
(33) MXQET.DOC, available from the University of California (San Diego) Supercomputer Center, along with the MXQET program itself.
(34) Hare Research Inc., 14810 216th Ave. NE, Woodinville, WA 98072.
(35) Dudewicz, E. J.; Mishra, S. N. *Modern Mathematical Statistics*; John Wiley and Sons: New York, 1988.
(36) Abragam, A. *The Principles of Nuclear Magnetism*; Oxford University Press: Oxford, 1961.
(37) Spiess, H. W. *Adv. Polym. Sci.* **1985**, *66*, 23.
(38) Wittebort, R. J.; Olejniczak, E. T.; Griffin, R. G. *J. Chem. Phys.* **1987**, *86*, 5411.

and [9,10-d_2]-C_{18}-silica (II)

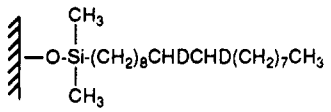

II

The peaks in Figure 1 that are labeled "experimental" show the room temperature ^2H NMR spectra of high-loading and low-loading [1,1-d_2]-C_{18}-silicas (I) in the presence and absence of saturation with liquids for quadrupole echo delay periods (τ) of 50 and 200 μs. Figure 2 shows an analogous set of spectra of the [9,10-d_2]-C_{18}-silicas (II). All these deuterium line shapes are in the general shape of a rounded triangle. The one room temperature line shape that is an exception to the pattern of triangular line shapes is that of the high-loading-level [9,10-d_2]-C_{18}-silica sample in the presence of cyclohexane, which shows a splitting of 10 kHz.

The full width at half-maximum (fwhm) for each room temperature ^2H spectrum, along with the ratio (I^{200}_{50}) of the peak height acquired with a τ value of 200 μs to the corresponding τ = 50 μs intensity, are given in Table II. The low-loading [1,1-d_2]-C_{18}-silica sample exhibits the broadest pattern observed in these spectra of samples at 25 °C. The addition of liquids to the low-loading C_{18}-silica results in a decrease of the fwhm in all cases, though the addition of solvents to the high-loading C_{18}-silicas does not narrow the spectra so dramatically as for the low-loading C_{18}-silicas.

The I^{200}_{50} results for the 25 °C C_{18}-silica samples vary from 0.76 to 0.44. I^{200}_{50} values that are greater than about 0.5, combined with the obvious motional narrowing of all of the ^2H line shapes at 25 °C, indicate that the C–D internuclear vectors undergo reorientation at rates near the upper limit of the "intermediate-motion" regime, which is 10^6 s^{-1} in this case.[39] In the case of either of the low-loading samples, the I^{200}_{50} value increases when the C_{18}-silicas are saturated with a liquid; but no such general trend is observed for the case of the high-loading C_{18}-silica samples.

In order to investigate the nature of the motion that leads to the line shapes observed in the 25 °C spectra, a series of wide-line ^2H spectra were obtained at reduced temperatures on the high-loading and low-loading [1,1-d_2] samples in the absence of wetting liquids. These spectra, labeled as the experimental spectra in Figure 3, indicate that, at −125 °C, both the high-loading and low-loading [1,1-d_2]-C_{18}-silica samples exhibit nearly static ^2H line shapes. As the temperature is raised to −100 °C for the low-loading sample and −75 °C for the high-loading sample, the ^2H resonance appears as a "flat-topped" peak, a behavior that has been observed previously in the ^2H NMR spectra of long-chain alkanes; Huang et. al.,[40] Jelinski et. al.,[41] and Ebelhauser and Spiess[42] have attributed this behavior to a two-site jump through an angle of 109.5° with unequal populations of the two jump sites. Hirschinger et al. attributed similar flat-topped patterns to a complex librational motion with a Gaussian distribution of libration amplitudes.[43] Figure 3 shows that, with further increases in temperature, a portion of the C_{18} chains exhibit the type of motion that is characterized by the rounded triangular patterns observed in the ^2H NMR spectra acquired at 25 °C. In the temperature range of −50 to +25 °C, both the broad line shape and the narrower triangular line shape appear in the ^2H NMR spectrum simultaneously; with increasing temperature, the relative contribution of the narrower triangular peak increases.

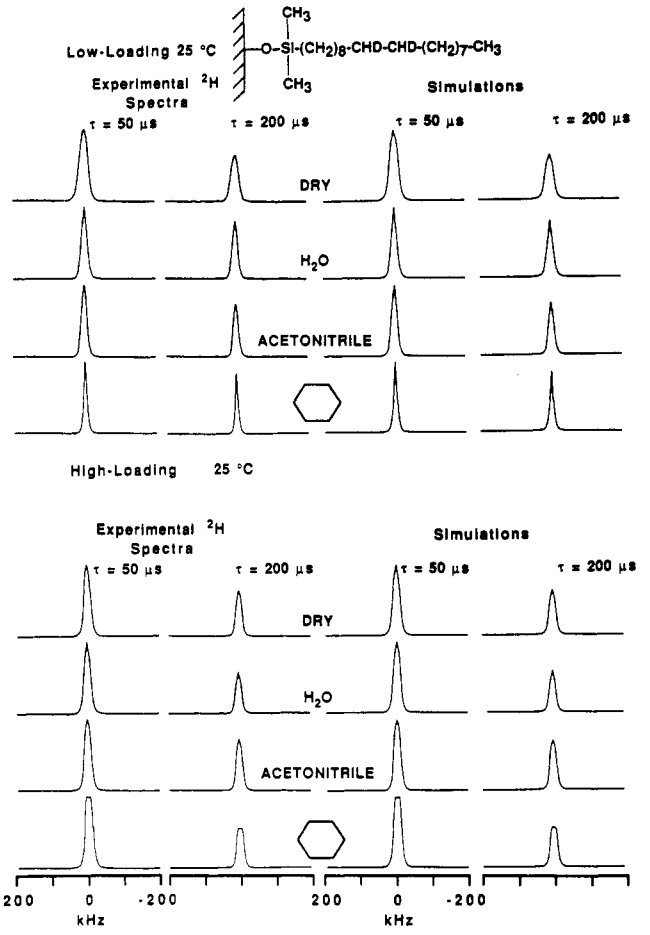

Figure 2. Comparison of simulated ^2H NMR spectra with the experimental spectra of low-loading and high-loading [9,10-d_2]-C_{18}-silica taken at room temperature. The parameters for these simulations can be found in Table VII.

Table II. Experimental Parameters Measured from ^2H Spectra of C_{18}-Silica (Figure 1) Taken at 25 °C

	[1,1-d_2]-C_{18}-silica			[9,10-d_2]-C_{18}-silica		
added liquid	τ[a] (μs)	fwhm[b] (kHz)	I^{200}_{50}[c]	τ[a] (μs)	fwhm[b] (kHz)	I^{200}_{50}[c]
		Low-Loading Sample[d]				
dry	50	47.6		50	27.6	
	200	44.8	0.53	200	25.6	0.42
H_2O	50	32.8		50	18.8	
	200	31.2	0.62	200	17.6	0.80
CH_3CN	50	36.8		50	18.0	
	200	32.0	0.76	200	16.4	0.72
C_6H_{12}	50	36.4		50	9.4	
	200	34.4	0.68	200	9.0	0.83
		High-Loading Sample[e]				
dry	50	33.6		50	21.6	
	200	30.0	0.44	200	19.6	0.62
H_2O	50	28.4		50	22.0	
	200	25.2	0.46	200	19.6	0.57
CH_3CN	50	30.8		50	22.4	
	200	26.0	0.49	200	20.8	0.69
C_6H_{12}	50	26.0		50	24.8	
	200	24.0	0.59	200	23.2	0.54

[a] Delay period in quadrupole echo experiment. [b] Full width at half-maximum of each ^2H resonance. [c] Ratio of ^2H peak intensity at τ = 200 μs to the intensity at τ = 50 μs. [d] Loading level of [1,1-d_2], 69 mg/g; loading level of [9,10-d_2], 70 mg/g. [e] Loading level of [1,1-d_2], 195 mg/g; loading level of [9,10-d_2], 218 mg/g.

^2H spectra were obtained at −50 °C for all of the deuterated C_{18}-silica samples in both the presence and absence of liquids; these spectra are shown as the experimental spectra in Figure 4. These spectra in general show less motional narrowing for the high-

(39) Spiess, H. W. *Colloid Polym. Sci.* **1983**, *261*, 193.
(40) Huang, T. H.; Skarjune, R. P.; Wittebort, R. J.; Griffin, R. J.; Oldfield, E. *J. Am. Chem. Soc.* **1980**, *102*, 7377.
(41) Jelinski, L. W.; Dumais, J. J.; Engel, A. K. *Macromolecules* **1983**, *16*, 492.
(42) Ebelhauser, R.; Spiess, H. *Ber. Bunsen-Ges. Phys. Chem.* **1985**, *89*, 1208.
(43) Hirschinger, J.; Miura, H.; Gardner, K. H.; English, A. D. *Macromolecules* **1990**, *23*, 2153.

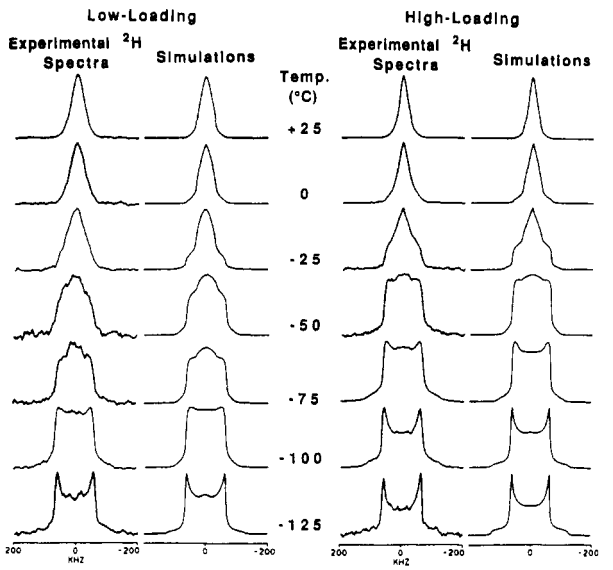

Figure 3. Comparison of simulated ^2H NMR spectra with the experimental spectra (τ = 50 μs) of dry low-loading and dry high-loading [1,1-d_2]-C_{18}-silica samples taken over a range of temperatures. The parameters for these simulations can be found in Table III.

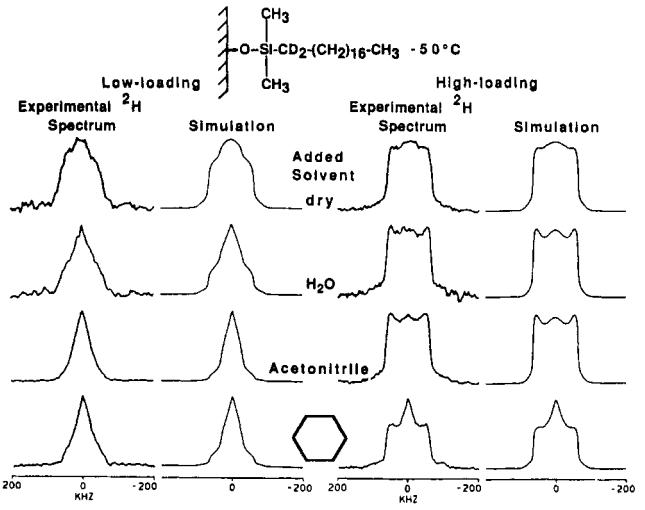

Figure 4. Comparison of simulated ^2H NMR spectra with the experimental spectra (τ = 50 μs) of low-loading and high-loading [1,1-d_2]-C_{18}-silica taken at −50 °C. The parameters for these simulations can be found in Table IV.

loading samples than for the low-loading samples.

Motional Models for C_{18}-Silica. In order to characterize in more detail the specific types of motion that could lead to the ^2H line shapes observed for the C_{18}-silica samples, it is necessary to compare these line shapes to those that result from computations based on a reasonable motional model for the C_{18}-silica system. Of course, an alternative approach could be based on the concept of "order parameters"; this approach was not explored in this study, except via the parameter P_g(width) introduced below.

Two-Site Jump Model. The first motional model explored for describing the ^2H data presented in the figures is illustrated in Figure 5; it is the "kink-3-bond" motion, which has been used to describe motions in polymers,[41] lipid bilayers,[44] and polymer model membranes.[42] This two-site exchange model adequately describes the broad resonances observed in the low-temperature spectra of C_{18}-silicas, those from −125 °C to near −50 °C. The specific motion described by this model is the trans–gauche reorientation

(44) Griffin, R. G. *Methods Enzymol.* **1981**, *72*, 108.
(45) Iler, R. K. *The Chemistry of Silica: Solubility, Polymerization, Colloid and Surface Properties, and Biochemistry*; John Wiley and Sons: New York, 1979.

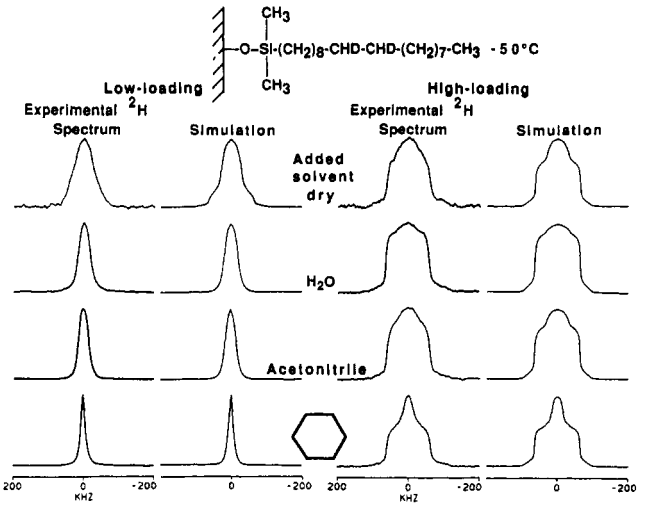

Figure 5. Comparison of simulated ^2H NMR spectra with the experimental spectra (τ = 50 μs) of low-loading and high-loading [9,10-d_2]-C_{18}-silica taken at −50 °C. The parameters for these simulations can be found in Table V.

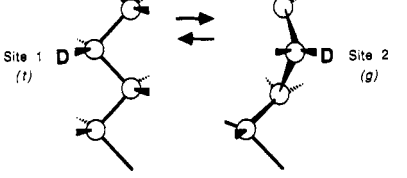

Figure 6. Example of a deuterium nucleus on an alkyl chain that is moving with a kink-3-bond motion.

of the C–^2H pair in which one of the orientations is more favorable because of steric interactions and is therefore more highly populated than the other orientation.

The kink-3-bond motion was implemented as the "two-site jump" computational model.[44] This model includes two orientations (or sites) that are related to each other by a tetrahedral "jump" angle (109.5°). The more highly populated trans site has population P_t, while the gauche site has population P_g. The following relationship applies to this and all subsequent motional models discussed in this paper:

$$P_g \leq P_t \tag{2}$$

Motional Model Based on a Distribution of P_g Values (Dist P_g Model). Equation 1 shows that a C–^2H system that is moving with a single geometry of motion and at a frequency greater than 10^6 Hz will exhibit a line shape that is the sum or a pair of motionally averaged patterns for the pair of ^2H NMR transitions (−1 ↔ 0 and 0 ↔ 1) corresponding to an η value between 0 and 1.[38] A homogeneous collection of uniformly averaged C–^2H patterns of this type will not yield the triangular patterns observed for the C_{18}-silica samples reported here. Hence, it appears that, at room temperature, the alkyl chains of C_{18}-silica move with an inhomogeneous *distribution* of geometries. Since silica surfaces are known to be inhomogeneous,[45] it appears reasonable to assume that C_{18}-silane groups are bound to a variety of different structures on the silica surface and therefore exhibit a variety of motions.

The C_{18}-silane chains of C_{18}-silica are bonded at one end only, and it seems reasonable to relate the motion of this system to that of a similarly constrained system. One example of such a system was studied in depth by Ebelhauser and Spiess.[42] In their study of the dynamics of alkyl chains in a polymer model membrane, they proposed a motional model that we will refer to as the "alkyl chain rotational jump" model.

Given the premise of a distribution of motions on the silica surface, a motional model for the C_{18}-silica system can be developed that is based on the alkyl chain rotational jump model

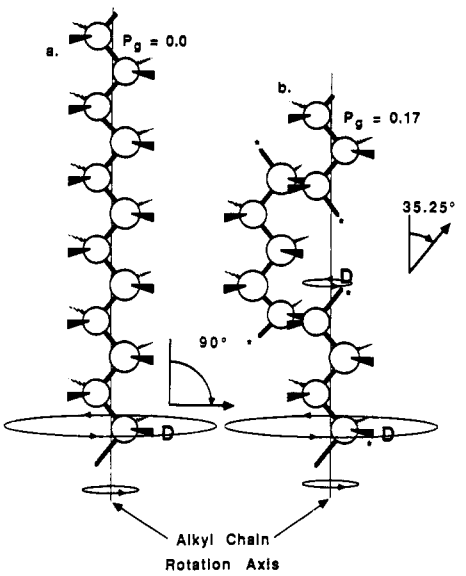

Figure 7. Motional basis for the alkyl chain rotational jump model, shown for two different chain conformations: (a) alkyl chain rotational jump for an alkyl chain with an all-trans conformation ($P_g = 0$) (b) alkyl chain rotational jump involving gauche conformers ($P_g > 0$).

but incorporating the effect of a variety of silica surface environments on the motion. Referring to Figure 7, it is apparent that, as rapid alkyl chain rotational jumps take place about the alkyl chain axis, the C_{18} chains that exhibit high P_g values must sweep out a larger effective volume than C_{18} chains exhibiting low P_g's. It follows that those C_{18} chains that are in a sterically less restrained environment on the inhomogeneous C_{18}-silica surface might exhibit greater values of P_g than those C_{18} chains in the more crowded regions of the silica surface. Therefore, it is reasonable to assume that the C_{18}-silane moieties exhibit motion that is characterized by a distribution of specific motional parameters, each individual set of parameters being a function of the structural environment of that particular silica-bound C_{18}-silane group.

The alkyl chain rotational jump model produces a line shape in the fast-motional limit ($\Omega > 1 \times 10^7$ Hz) that has a line width that is dependent on P_g. The effective, motionally scaled quadrupolar coupling constant (QCC_{scaled}) of the Pake pattern observed in the fast-motion limit for the alkyl chain rotational jump model varies with P_g and the static quadrupole coupling constant (QCC) according to the following equation:[38]

$$QCC_{scaled} = QCC(0.5 - P_g) \tag{3}$$

A heterogeneous "distribution of P_g's model", or "dist P_g model", was implemented by choosing a distribution function, such as a Gaussian distribution or a γ distribution, to approximate a distribution of P_g values that could exist on the C_{18}-silica surface. The free induction decays resulting under the influence of C_{18} chain motion at Ω values of 1×10^7 Hz or greater were calculated for 42 different values of P_g. A computer routine then summed the individual free induction decays that result from a C_{18} chain under the alkyl chain rotational jump motion as characterized by a given P_g value, with their contributions scaled according to the distribution function chosen to approximate the P_g distribution. After the normalized sum of the FID's was taken, the resulting summed FID was Fourier-transformed to yield the simulated ^2H NMR spectrum that corresponds to that particular distribution of P_g values.

The room temperature ^2H NMR spectra of the [1,1-d_2]-C_{18}-silica samples shown in Figure 1 exhibit a broad component that, within this strategy, requires a simulation that employs a distribution of P_g values that is asymmetrical about the maximum P_g value, P_g(max), and skewed toward lower P_g values. A γ distribution[35] was chosen to represent this skewed distribution. The fraction of C_{18} chains characterized by each P_g value, $f(P_g)$,

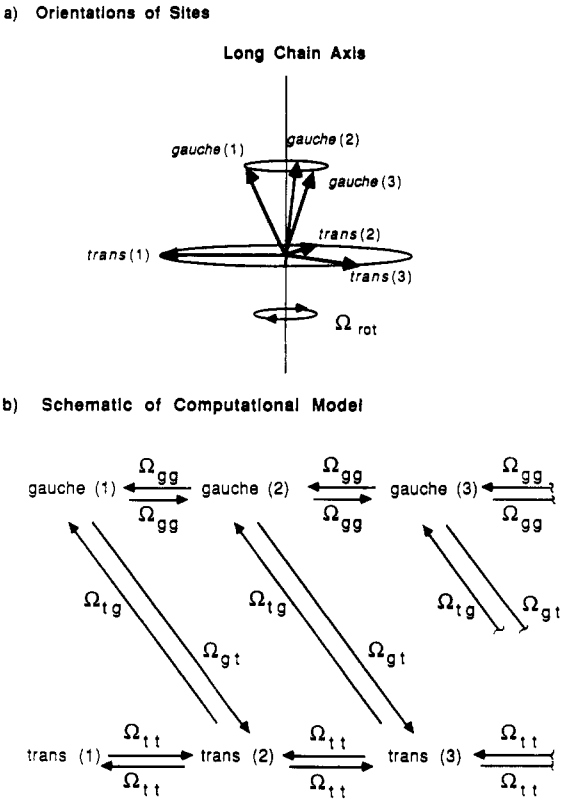

Figure 8. Illustration of the alkyl chain rotational jump model: (a) Orientations of the various sites in the model (b) schematic diagram of the kinetic framework of the computer simulation. In each simulation described in this paper, all Ω values were set equal to one another ($\Omega_{gg} = \Omega_{gt} = \Omega_{tt}$).

for the [1,1-d_2]-C_{18}-silicas is determined in the dist P_g model simulated by the following equation for a γ distribution:

$$f(P_g) = C(x^r)[\exp(-x/d)] \tag{4}$$

where

$$x \equiv 0.5 - P_g \tag{5}$$

and r and d were empirically determined to reproduce each ^2H line shape. The alkyl chain rotational jump model limits the possible values of P_g to those between 0 and 0.5. The constant C was used to normalize the distribution.

The 25 °C ^2H NMR spectra of the [9,10-d_2]-C_{18}-silica samples shown in Figure 2 do not exhibit the broad component at the base of the NMR resonances shown in the spectra of the [1,1-d_2]-C_{18}-silicas. The P_g distribution that best reproduced the experimental line shapes of the [9,10-d_2]-C_{18}-silica samples is the Gaussian distribution:[35]

$$f(P_g) = C\{\exp[-(P_g - P_g(\max))^2/2\sigma^2]\} \tag{6}$$

where C is a normalizing constant and P_g(max) and σ define the position and width of the Gaussian distribution, respectively.

Three parameters that characterize the dist P_g model simulation of a ^2H NMR spectrum can be related to the C_{18}-silica structure. The first of these parameters is the P_g value that represents the largest population in the chosen P_g distribution, "P_g(max)". In the dist P_g model, the value of P_g(max) should be governed by the motional freedom of the C_{18} chain at the deuteration site, since the effective volume required for the C_{18} chains to rotate is larger with a larger value of P_g.

The second structural parameter that describes a given dist P_g model simulation is the full width at half-maximum of the distribution function chosen, "P_g(width)". The value of P_g(width) should provide a measure of the degree of order on the C_{18}-silica surface, since a hypothetical, perfectly ordered C_{18}-silica system

Table III. Parameters Used To Simulate Low-Temperature ^2H NMR Spectra (Figure 3) of Dry [1,1-d_2]-C_{18}-Silica Samples

temp (°C)	two-site jump parameters			dist P_g model parameters		
	%[a]	P_g[b]	Ω (MHz)[c]	%[a]	n[d]	d[d]
Low-Loading [1,1-d_2]-C_{18}-Silica[e]						
−125	100.0	0.0	0.3	0.0		
−100	100.0	0.0	5.0	0.0		
−75	94.4	0.2	5.0	5.6	1.0	1000
−50	87.0	0.2	7.0	13.0	1.0	1000
−25	45.5	0.2	7.0	54.5	0.9	1000
0	9.1	0.2	7.0	90.9	0.7	1000
25	0.0			100.0	1.0	0.44
High-Loading [1,1-d_2]-C_{18}-Silica[f]						
−125	100.0	0.0	0.1	0.0		
−100	100.0	0.0	0.3	0.0		
−75	98.0	0.2	5.0	2.0	1.0	1000
−25	71.4	0.2	7.0	28.6	0.5	1000
0	20.0	0.2	7.0	80.0	0.8	0.5
25	0.0			100.0	1.2	0.16

[a] Percent ^2H nuclei described by each motional model contributing to total line shape. [b] Fraction of gauche site occupation in two-site jump model. [c] gauche to trans jump rate in two-site jump model. [d] Parameters describing the γ distribution. See eqs 4 and 5. [e] 69 mg/g loading level. [f] 195 mg/g loading level.

should have the same P_g value for all of the surface-bound C_{18} chains. The spectrum of such a system should appear as a "standard" Pake pattern, and the P_g(width) value for this hypothetical, perfectly ordered system would be 0. This argument suggests that a value of P_g(width) that is greater than 0 is an indicator of dispersion in the structural/motional modes of the silica-bound C_{18} chains.

The third parameter characteristic of a given dist P_g model simulation is Ω, the rate of motional jumps in the alkyl chains of the C_{18}-silica surface. Since the dist P_g model simulations are based on ^2H line shapes that are in the fast motional limit, it is not possible to determine Ω from any single line shape simulation using the dist P_g model. However, it is possible to obtain information on Ω from the simulations of two different ^2H spectra of the same sample that are taken at different quadrupole echo delay periods (vide infra).

Low-Temperature Spectra of [1,1-d_2]-C_{18}-Silicas. The low-temperature ^2H NMR spectra of the high-loading and low-loading dry [1,1-d_2]-C_{18}-silicas were simulated by line shapes that are each a *sum of two contributions*: (a) a line shape resulting from a two-site jump model to simulate the broad component of the ^2H spectrum and (b) a line shape from a dist P_g model simulation to reproduce the narrower, triangular resonance of the ^2H spectrum. The simulated line shapes for the high-loading and low-loading [1,1-d_2]-C_{18}-silica spectra are compared to the corresponding experimental ^2H spectra in Figure 3, and the parameters used in these simulations are summarized in Table III.

The simulations corresponding to the spectra of the high-loading [1,1-d_2]-C_{18}-silica samples show that, at a temperature of −125 °C, there is little motion of the C–^2H bond and a static Pake pattern describes this line shape well. At sample temperatures less than −50 °C, the observed line shapes are simulated satisfactorily by the two-site jump model. At −50 °C, a small contribution due to the "triangular" line shape simulated by the dist P_g model seems to be present. From −50 to +25 °C, the fraction of the ^2H peak area that is simulated with the dist P_g model increases from 2% to 100% and the fraction that is characterized by the two-site jump model correspondingly decreases. The most likely explanation for the presence of two types of motion in the C_{18}-silica sample in the temperature range of −50–0 °C is that those C_{18} chains that are sterically crowded on the silica surface move with the sterically more restricted two-site motion, while those C_{18} chains with a greater available volume in which to move execute a more random motion characterized by the dist P_g model. On the basis of this conjecture, one would expect that, at a given temperature, a greater percentage of C_{18} chains that exhibit the more random motion should exist on the less crowded, low-loading C_{18}-silica surface than on a high-loading C_{18}-silica sample; the data for the high-loading and low-loading C_{18}-silicas in Table III provide support for this view. The simulations for the low-loading and high-loading C_{18}-silica samples show that both samples exhibit motions that are nearly identical in *type* but that the low-loading C_{18}-silica has a higher percentage of more randomly moving C_{18} chains at any given temperature.

Table IV. Parameters Used to Simulate −50 °C ^2H NMR Spectra (Figure 4) of [1,1-d_2]-C_{18}-Silica Samples with and without Solvents Added

added liquid	two-site jump parameters			dist P_g model		
	%[a]	P_g[b]	Ω (MHz)[c]	%[a]	n[d]	d[d]
Low-Loading [1,1-d_2]-C_{18}-Silica[e]						
dry	87.0	0.2	7.0	13.0	1.0	1000
H_2O	66.7	0.2	10.0	33.3	0.5	1000
CH_3CN	25.0	0.2	10.0	0.75	0.5	1000
C_6H_{12}	40.0	0.2	10.0	60.0	0.5	1000
High-Loading [1,1-d_2]-C_{18}-Silica[f]						
dry	98.0	0.2	5.0	2.0	1.0	1000
H_2O	99.0	0.2	3.0	1.0	1.0	1000
CH_3CN	100.0	0.2	3.0	0.0		
C_6H_{12}	90.9	0.2	5.0	9.1	1.1	0.13

[a] Percent ^2H nuclei described by each motional model contributing to total line shape. [b] Fraction of gauche site occupation in two-site jump model. [c] gauche to trans jump rate in two-site jump model. [d] Parameters describing the γ distribution. See eqs 4 and 5. [e] 69 mg/g loading level. [f] 195 mg/g loading level.

^2H NMR Spectra of C_{18}-Silica Obtained at −50 °C. The suggestion that the percentage of C_{18} chains moving with the more random motion characterized by the dist P_g model increases with the average steric freedom of motion in C_{18}-silica was examined in terms of the effects of added liquids. Combinations of a line shape from a two-site jump model simulation and a line shape from a dist P_g model simulation were used to calculate the theoretical line shapes for these spectra. The results shown in Figure 4 and Table IV suggest that, in the case of the low-loading [1,1-d_2]-C_{18}-silica samples, the highest percentage of the more randomly moving, and therefore more sterically demanding, C_{18} chains is in the sample with added acetonitrile. For the low-loading C_{18}-silica samples, cyclohexane, and to a lesser extent water, also increases the percentage of the more randomly moving component when they are added.

The high-loading [1,1-d_2]-C_{18}-silica samples are described in terms of a lower percentage of the more random C_{18} chain motion than their low-loading [1,1-d_2] counterparts. The simulation results summarized in Figure 4 and Table IV show that the addition of water or acetonitrile to the high-loading [1,1-d_2]-C_{18}-silica sample decreases Ω slightly at −50 °C. The percentage of C_{18} chains exhibiting the more random motion is 2% or less for the dry sample and for the sample with water or acetonitrile present. For the addition of cyclohexane to the high-loading [1,1-d_2]-C_{18}-silica, the component of motion described by the dist P_g motion model must be increased to 9.1% for a good fit, indicating that the addition of cyclohexane increases the motion of a small fraction of the anchored ends of the C_{18} chains in the high-loading C_{18}-silica.

The ^2H nuclei in the [9,10-d_2]-C_{18}-silicas are located farther from the rigid silica matrix, so it is reasonable that, at −50 °C, the ^2H spectra obtained on these nuclei should exhibit a higher percentage of the more random motion characterized by the dist P_g model than do the corresponding [1,1-d_2]-C_{18}-silica samples. Figure 5 and Table V show the spectra simulated to match the ^2H spectra of these samples and the corresponding simulation parameters. The spectrum of the dry, low-loading [9,10-d_2]-C_{18}-silica sample was best simulated by a combination of 37% C_{18} chains moving by the dist P_g model plus 63% moving by the two-site jump model. Upon addition of liquid to this low-loading [9,10-d_2]-C_{18}-silica, the observed resonances are well simulated by the dist P_g model alone. The P_g(max) values reported for the low-loading [9,10-d_2]-silicas in Table V suggest that cyclohexane

Table V. Parameters Used To Simulate −50 °C ^{2}H NMR Spectra (Figure 4) of [9,10-d_2]-C_{18}-Silica Samples with and without Solvents Added

added liquid	two-site jump parameters			dist P_g model parameters		
	%[a]	P_g[b]	Ω (MHz)[c]	%[a]	P_g (max)	P_g(width)[e]
	Low-Loading [9,10-d_2]-C_{18}-Silica[f]					
dry	37.0	0.2	10.0	63.0	0.1	0.17
H_2O	0.0			100.0	0.24	0.11
CH_3CN	0.0			100.0	0.29	0.10
C_6H_{12}	0.0			100.0	0.42	0.10
	High-Loading [9,10-d_2]-C_{18}-Silica[g]					
dry	84.7	0.2	7.0	15.3	0.1	0.17
H_2O	95.0	0.2	7.0	5.0	0.15	0.16
CH_3CN	89.0	0.2	7.0	11.0	0.1	0.17
C_6H_{12}	87.0	0.2	7.0	13.0	0.3	0.18

[a] Percent H nuclei described by each motional model contributing to total line shape. [b] Fraction of gauche site occupation in two-site jump model. [c] gauche to trans jump rate in two-site jump model. [d] Center of Gaussian distribution of P_g values. See eq 6. [e] Full width at half-maximum of Gaussian distribution of P_g values, equal to 2.355σ. See eq 6. [f] Loading level, 70 mg/g. [g] Loading level, 218 mg/g.

Table VI. γ Distribution Parameters Used To Simulate 25 °C ^{2}H NMR Spectra (Figure 1) of [1,1-d_2]-C_{18}-Silica Samples

added liquid	τ (μs)	n[a]	d[a]	P_g(max)	P_g(width)[b]
	Low-Loading [1,1-d_2]-C_{18}-Silica[c]				
dry	50	1.0	0.44	0.060	0.398
	200	1.1	0.29	0.181	0.420
H_2O	50	0.8	0.26	0.292	0.461
	200	0.9	0.205	0.315	0.461
CH_3CN	50	0.9	0.27	0.257	0.449
	200	1.0	0.18	0.320	0.440
C_6H_6	50	0.9	0.26	0.266	0.451
	200	1.0	0.21	0.290	0.451
	High-Loading [1,1-d_2]-C_{18}-Silica[d]				
dry	50	1.2	0.16	0.308	0.426
	200	1.4	0.115	0.339	0.329
H_2O	50	0.95	0.177	0.332	0.423
	200	1.0	0.145	0.355	0.355
CH_3CN	50	1.05	0.18	0.311	0.450
	200	1.1	0.13	0.357	0.332
C_6H_6	50	1.1	0.13	0.357	0.332
	200	1.5	0.115	0.368	0.300

[a] Parameters describing the γ distribution function used in each simulation. See eqs 4 and 5. [b] Full width at half-maximum of the γ distribution function used in each simulation. [c] Loading level, 69 mg/g. [d] Loading level, 195 mg/g.

is the most effective solvent for reducing steric hindrance to the C_{18} chain motion for the central portion of the C_{18} chains. The addition of water or acetonitrile apparently decreases the steric hindrance to C_{18} chain motion of the low-loading C_{18}-silica to a lesser degree than cyclohexane does.

As shown in Figure 5 and Table V, the ^{2}H line shape of the dry, high-loading [9,10-d_2]-C_{18}-silica at −50 °C does not change substantially upon the addition of water or acetonitrile. While the addition of cyclohexane does not appear to substantially change the fraction of C_{18} chains that are moving with the more random motion, it does narrow the line width representing the more randomly moving fraction of the C_{18} chains. The addition of cyclohexane to C_{18}-silica apparently decreases the steric hindrance to motion of that portion of the central segments of the C_{18} chains that are moving according to the dist P_g model but does not significantly affect the more motionally restrained fraction of the C_{18}-silica system that is moving with the two-site jump motion.

^{2}H NMR Spectra of [1,1-d_2]-C_{18}-Silica Obtained at 25 °C. The experimental 25 °C ^{2}H NMR spectra of the [1,1-d_2]-C_{18}-silica samples are shown in Figure 1 together with the line shapes fitted to these resonances with the dist P_g model. The parameters used to simulate these spectra can be found in Table VI, and the corresponding experimental $I^{200}{}_{50}$ values and fwhm values for these samples are reported in Table II.

Table VII. Gaussian Distribution Parameters Used To Simulate 25 °C ^{2}H NMR Spectra (Figure 2) of [9,10-d_2]-C_{18}-Silica Samples

added liquid	τ (μs)[a]	P_g(max)[b]	P_g(width)[c]
	Low-Loading [9,10-d_2]-C_{18}-Silica[d]		
dry	50	0.305	0.212
	200	0.320	0.200
H_2O	50	0.367	0.200
	200	0.368	0.193
CH_3CN	50	0.365	0.170
	200	0.375	0.160
C_6H_{12}	50	0.423	0.212
	200	0.427	0.212
	High-Loading [9,10-d_2]-C_{18}-Silica[e]		
dry	50	0.347	0.177
	200	0.355	0.165
H_2O	50	0.351	0.165
	200	0.365	0.165
CH_3CN	50	0.355	0.153
	200	0.359	0.151
C_6H_{12}	50	0.341	0.141
	200	0.348	0.136

[a] Quadrupole echo delay period. [b] Maximum of Gaussian distribution of P_g values. See eq 6. [c] Full width at half-maximum of the Gaussian distribution of P_g values, equal to 2.355σ. See eq 6. [d] Loading level, 70 mg/g. [e] Loading level, 218 mg/g.

Referring to the fwhm values for the τ = 50 μs data in Table II, one sees that these values for all of the [1,1-d_2]-C_{18}-silica samples, except the low-loading dry sample, fall into the range of 26–37 kHz. The stated exception to this range has a fwhm value of 47.6 kHz. These results show that the C_1 carbons of the C_{18} chains are much more restricted in motion in the case of a low-loading dry C_{18}-silica than in the case of the higher loading C_{18}-silicas or C_{18}-silicas with solvents present on the surface.

The full width of the P_g distribution (at half-maximum height), denoted above as P_g(width), is reported for each [1,1-d_2]-C_{18}-silica spectrum in Table VI. It is difficult to interpret the P_g(width) values in a simple manner for the low-loading [1,1-d_2]-C_{18}-silica samples, because of the nature of the alkyl chain rotational jump model that provides the basis for the Pake patterns used in the dist P_g model. Of course, the minimum P_g value that is physically possible in the alkyl chain rotational jump model is 0. Referring to eq 3, one can see that restricting P_g to values greater than 0 restricts the maximum values of QCC_{scaled} of the Pake patterns that are components of the dist P_g model simulation to no more than half of the QCC value corresponding to the case of a static Pake pattern. All of the simulated spectra presented here were calculated by using only Pake patterns with values of QCC_{scaled} that range from 2 kHz (corresponding to a P_g value of 0.488) to 84 kHz (which corresponds to a P_g value of 0). These truncated distribution functions exhibit anomalously small P_g(width) values when they are compared to the distribution functions describing the other ^{2}H line shapes, so it is misleading to compare the P_g-(width) values for the low-loading [1,1-d_2]-C_{18}-silica to those for the other samples, and such comparisons should be avoided.

Separate distribution functions are reported for the ^{2}H line shapes at τ values of 50 and 200 μs for each sample in Tables VI and VII. The nature of these fits is consistent with the premise of the dist P_g model, since the C_{18}-silica groups that move relatively slowly should be characterized by relatively small $I^{200}{}_{50}$ values and would therefore be represented by a smaller contributing population to the resonance at τ = 200 μs than for the case of τ = 50 μs. The basic assumption behind the dist P_g model is that the broader components of the observed ^{2}H line shapes correspond to small P_g values and represent C_{18}-silica species that are in a relatively constrained environment. It is reasonable that such a species move more slowly than its less constrained neighbors. In nearly every case in Tables VI and VII, the distribution function that describes the τ = 200 μs line shape has a P_g(max) value that is larger than the distribution function that describes the corresponding τ = 50 μs line shape. Therefore, the observed ^{2}H line shapes are consistent with the hypothesis that the slower moving components in the ^{2}H line shapes correspond to those that are

characterized by small P_g values.

In the case of the high-loading [1,1-d_2]-C_{18}-silica samples, the significance of the P_g(width) values is clear, since the half-maximum intensities of the γ distributions used to fit the spectra of these samples all fall within the P_g range of 0.0–0.5. The P_g(width) value for the high-loading [1,1-d_2]-C_{18}-silica sample saturated with cyclohexane is about 25% lower than P_g(width) for the other samples. This result shows that cyclohexane introduces order into that portion of the C_{18}-silica system that is close to the silica surface. This introduction of order suggests that cyclohexane acts as an "annealing" agent for the high-loading C_{18}-silica system and that cyclohexane is effective for relieving the strain and disorder that exists in the C_{18} chains near the silica anchor of the high-loading C_{18}-silica.

^{2}H NMR Spectra of [9,10-d_2]-C_{18}-Silica Obtained at 25 °C. The experimental ^{2}H spectra of all of the [9,10-d_2]-C_{18}-silica samples studied, along with spectra simulated by the dist P_g model for each case, are illustrated in Figure 2. Values of P_g(max) and the P_g(width) used in the simulations for the [9,10-d_2]-C_{18}-silica samples at 25 °C are summarized in Table VII. Referring to the values of fwhm for the τ = 50 μs cases in Table II, it is clear that the fwhm value for the dry low-loading [9,10-d_2]-C_{18}-silica sample is about 20% greater than those for any of the other [9,10-d_2]-C_{18}-silicas. Inspection of the results summarized in Table VII reveals that this increase in the fwhm is reflected in the ^{2}H simulations of these spectra as a decrease of about 20% in the P_g(max) values of the dry low-loading [9,10-d_2]-C_{18}-silica sample relative to the other [9,10-d_2]-C_{18}-silica samples. This high fwhm value and the low P_g(max) value indicate that the readily achievable configurations and motion of the central portion of the C_{18} chains of the dry low-loading C_{18}-silica are more restricted than those exhibited by the C_{18} chains upon the addition of solvents or upon increasing the surface silyl loading level. The relatively small values of P_g(width) associated with the [9,10-d_2]-C_{18}-silica samples imply that the 9,10-position of the C_{18} chains in low-loading C_{18}-silica is more highly ordered than the 1,1-position. The addition of solvents to the low-loading [9,10-d_2]-C_{18}-silica samples decreases the fwhm value and raises the value of P_g(max), again indicating that solvent addition increases the freedom of the C_{18} chains to move.

In the case of the high-loading [9,10-d_2]-C_{18}-silyl silica experiments with τ = 50 μs, a small quantity of H_2O or CH_3CN has no observable effect on the C_{18} chain mobility as observed by the fwhm values reported in Table II and the values of P_g(max) in Table VII. However, the addition of cyclohexane actually increases the fwhm value and decreases the value of P_g(max), and therefore appears to decrease the mobility of the C_{18} chains. The P_g(width) values are seen in Table VII to decrease with the addition of liquids, and the magnitude of P_g(width) is lower with decreasing polarity of the solvent; the [9,10-d_2]-C_{18}-silica with added cyclohexane exhibits the lowest P_g(width) value for any C_{18}-silica sample observed in this study. This low value of P_g(width) appears along with the previously described splitting in the resonance pattern of the high-loading [9,10-d_2]-C_{18}-silica spectrum, since the distribution of P_g values is sufficiently narrow in this case that the Pake character of the ^{2}H pattern is directly apparent. This is more evidence that cyclohexane allows the C_{18} chains to "anneal" to a relatively ordered and homogeneous configuration in which the C_{18} chains are all in similar environments and orientations. A likely candidate for this ordered state would be a "brush configuration", in which the C_{18} chains are relatively straight and perpendicular to the silica surface.

Motional Rates in C_{18}-Silica at 25 °C. I^{200}_{50} values were used to estimate Ω for the C_{18}-silica samples at 25 °C. For each case, a line shape simulation based on the alkyl chain rotational jump model was run, by using a P_g value equal to the P_g(max) value from the dist P_g model simulation for that particular case at τ = 50 μs. Given the model and the value of P_g(max), it was necessary only to find the value of Ω that would lead to a simulated I^{200}_{50} value reported in Table II. The Ω values found in this way for all of the C_{18}-silica samples at 25 °C are reported in Table VIII.

Table VIII. Motional Rates (Ω) Estimated from 25 °C ^{2}H NMR Spectra of C_{18}-Silica Samples

added liquid	[1,1-d_2]-C_{18}-silica Ω (MHz)[a]	[9,10-d_2]-C_{18}-silica Ω (MHz)[a]
	Low-Loading Sample[b]	
dry	17	26
H_2O	29	49
CH_3CN	40	34
C_6H_6	37	48
	High-Loading Sample[c]	
dry	14	25
H_2O	14	15
CH_3CN	14	31
C_6H_6	20	17

[a] Calculated rate of C_{18} chain reorientation at given deuteration site as determined from simulations of the ^{2}H NMR spectra with quadrupole echo delays of τ = 50 μs and τ = 200 μs. [b] Loading level of [1,1-d_2], 69 mg/g; loading level of [9,10-d_2], 70 mg/g. [c] Loading level of [1,1-d_2], 195 mg/g; loading level of [9,10-d_2], 218 mg/g.

The Ω values reported here are based on the assumption that no other relaxation mechanism, such as dipolar relaxation, contributes significantly to the deuterium T_2 values and that only site exchange contributes to the dephasing of the deuterium signals. Since other contributions to the deuterium line shape are small compared to the quadrupolar line broadening, this seems to be a reasonable assumption. Nevertheless, these values should be taken as estimates of the minimum values of Ω.

The dry low-loading C_{18}-silica sample exhibits a Ω value of 17 MHz at C1, while the motional rate is greater at C9–C10, with an estimated Ω value of 26 MHz. These two Ω values differ by less than a factor of 2, indicating that there is no dramatic difference in the motional rate between those carbons near the silica-anchored ends of the C_{18} chains and those midway along the chains. The addition of water, acetonitrile, or cyclohexane to the low-loading samples increases the estimated value of Ω by about a factor of 2 for both the anchored ends of the C_{18} chains and the central portions of the chains. This result indicates that all of these liquids increase the C_{18} chain mobilities.

The results summarized in Table VIII show that, in the case of the high-loading [9,10-d_2]-C_{18}-silica samples, the estimated Ω for the C_{18} chains increases upon the slight addition of acetonitrile. For the 9,10-portion of the C_{18} chains, the addition of water or cyclohexane decreases the average value of Ω. This decrease in motional rate is easily rationalized for the case of added water, since the C_{18} chains are hydrophobic and the addition of water to the C_{18}-silica surface could result in a concentration of the C_{18} chains into a "phase" that is separate from the water-adsorbed surface. If this formation of a separate phase occurs, perhaps in either a brushlike or a "haystack" configuration, then the C_{18} chains will be forced together by the hydrophobic behavior, and therefore the motional rates characterized by Ω could be decreased.

The decrease in the estimated value of Ω for the case of cyclohexane addition to the high-loading [9,10-d_2]-C_{18}-silica sample may come about as a result of the association of the cyclohexane molecules with the C_{18} chains. Cyclohexane molecules between the C_{18} chains would decrease the free volume available to each of the C_{18} chains and could therefore decrease the average value of Ω for the C_{18} chains. This decrease in free volume would be consistent with the small fwhm and P_g(max) values associated with the high-loading [9,10-d_2]-C_{18}-silica sample with added cyclohexane (since small values of P_g(max) can be associated with a relatively large degree of steric hindrance to the C_{18} chain motion). In contrast, the estimated Ω value is greater for the high-loading [1,1-d_2]-C_{18}-silica with cyclohexane present than for the dry high-loading [1,1-d_2]-C_{18}-silica. This increase of Ω for the 1,1-segment of the C_{18} chains near the silica surface may indicate that the cyclohexane is not present near the C1 position of the C_{18} chains. It is just as likely, however, that the annealing effect of cyclohexane that is observed most dramatically for the high-loading [9,10-d_2]-C_{18}-silica sample may relieve the most strained conformations of the C_{18} chains and thereby increase the

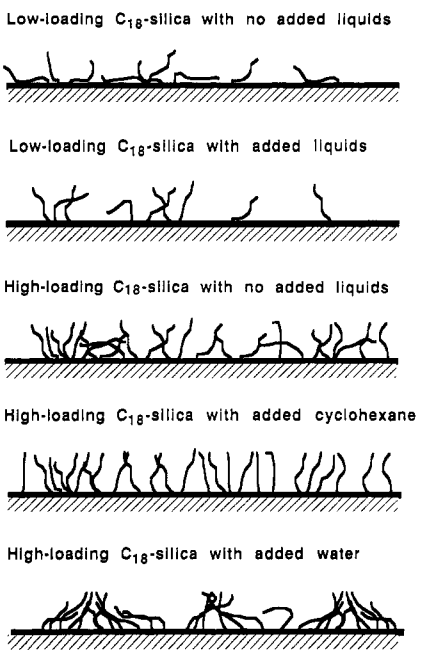

Figure 9. Some proposed structures of the C_{18}-silica surface.

average value of Ω near the silica surface.

Summary and Conclusions

The ^2H NMR results create a consistent picture of the motional characteristics of the C_{18}-silica system. Restricted C1 motion in the dry, low-loading [1,1-d_2]-C_{18}-silica suggests an unusually strong constraint of C_{18} chain motion in this sample, a constraint that is removed or alleviated either by the addition of solvents or by increasing the C_{18}-silane loading level. The most likely explanation of this unusual motional constraint is an interaction between the C_{18} chains and the silica surface, presumably of the van der Waal's type. As the density of the C_{18} chains on the surface is increased, the C_{18} chain motion could become less constrained because of the displacement of the C_{18} chains from the silica surface.

The ^2H NMR based view of the dry, low-loading C_{18}-silica system, with highly disordered C_{18} chains interacting strongly with the silica surface, is illustrated in Figure 9a. The addition of any of the solvents studied to the low-loading C_{18}-silica appears to displace the C_{18} chains from the silica surface because of either an interaction of the "liquid" molecules with the C_{18} chains in the case of a nonpolar liquid or replacement of the C_{18} chains on the silica surface in the case of a polar liquid and allows the C_{18} chains to exist in a wide variety of conformations, as depicted in Figure 9b. Since the C_{18} chains in the low-loading samples with added liquid are in rapid motion (30 MHz or more), there must be rapid reorientation of each C_{18} chain between many different configurations.

The major differences that were observed between samples with the two silane loading levels center on the fact that the high-loading samples are changed less by addition of liquids (albeit smaller amounts) than low-loading C_{18}-silica samples. The observed ^2H pattern for the high-loading [9,10-d_2]-C_{18}-silica sample with added cyclohexane shows that this sample is an unusually well ordered system in the region near the middle of the C_{18} chain. The corresponding [1,1-d_2]-C_{18}-silica/cyclohexane sample exhibits a ^2H line shape for which simulations indicate unusually rapid and random motion at the silica-anchored end of the C_{18} chain. These two observations suggest that the addition of cyclohexane to a high-loading C_{18}-silica sample allows the chains to assume a well-ordered configuration, such as the brush configuration depicted in Figure 9d, perhaps reducing the orientational/motional constraints on the C1 carbon that otherwise would exist when a larger fraction of the C_{18} chains are in strained orientations near the silica surface.

The ^2H NMR data on the sterically crowded high-loading C_{18}-silica samples (silane group packing of 1.3 monolayers, as calculated on the basis of a van der Waal's radius for a trimethylsilyl group) show that the C_{18} chains do not move as rapidly as in the case of the low-loading C_{18}-silica with solvents added. The high-loading C_{18}-silica samples all exhibit ^2H NMR results consistent with the picture in Figures 9c–e, in which a variety of C_{18} surface conformations occur, but in which very few of the conformations have methylene units interacting directly with the silica surface to a significant degree.

The low Ω values estimated from the motional-model simulation of the ^2H data for the high-loading C_{18}-silica sample with added H_2O suggest that the hydrophobic C_{18} chains may aggregate in this particular sample, so that the mobility of the C_{18} chains is impeded by interactions with other nearby C_{18} chains, as depicted for a haystack configuration[46] in Figure 9e.

The −50 °C ^2H line shape results on the C_{18}-silica system with various added liquids are very diverse. The ^2H spectra of the high-loading C_{18}-silica at −50 °C confirm the results of the 25 °C ^2H line shape studies, i.e., that cyclohexane is a particularly effective solvent for increasing the mobility of the C_{18} chains in the high-loading case.

Although the dist P_8 model used to simulate the ^2H data is not the only motional model that could describe the observed ^2H line shapes, it is evident that any model that can adequately account for both the ^2H line shapes and the response to variation in the quadrupole echo delay (τ) may involve a distribution of motions, suggesting a system with highly nonuniform structural/dynamical characteristics, as loosely represented in Figure 9. One example of another motional model that can describe ^2H line shapes similar to those observed in C_{18}-silicas was developed by Hirschinger et al. to describe the ^2H line shapes observed in highly constrained polymer systems.[43] Any realistic picture of the C_{18}-silica surface should most likely be a statistical model that encompasses a variety of surface structures, with the precise nature and population of each type dependent on the surface loading level and the presence or absence of added liquids. In general, the results presented in this paper show that wide-line ^2H line shapes are extremely useful probes of the C_{18} chains in the C_{18}-silica system and, in conjunction with line shape simulations, permit one to examine both structure and dynamics. This approach shows exceptional promise for the study of the interactions of various substances with derivatized silica systems.

Acknowledgment. We gratefully acknowledge partial support of this work by NSF Grant CHE-8610151 and use of the Colorado State University Regional NMR Center, funded by National Science Foundation Grant No. CHE-8616437. We also thank Dr. Bruce Hawkins for his technical assistance.

(46) Karch, K.; Sebestian, I.; Halasz, I. *J. Chromatogr.* **1976**, *122*, 3.